Supplementary Information

for

Cyclam with a phosphinate-bis(phosphonate) pendant arm is a bone targeting carrier of copper radionuclides

Lucia Pazderová,[a] Martina Benešová,[a,b] Margareta Vojtíčková,[a] Jana Havlíčková,[a] Jan Kotek,[a] Přemysl Lubal,[c] Martin Ullrich,[d] Martin Walther,[d] Sabine Schulze,[e] Christin Neuber,[d] Stefan Rammelt,[f] Hans-Jürgen Pietzsch,[d,g] Jens Pietzsch,[d,g] Vojtěch Kubíček,[a]* Petr Hermann[a]

[a]Department of Inorganic Chemistry, Faculty of Science, Charles University, Hlavova 8, 128 40 Prague 2, Czech Republic. Tel.: +420221951436; fax: +420221951253; e-mail: kubicek@natur.cuni.cz

[b]Research Group Molecular Biology of Systemic Radiotherapy, German Cancer Research Center, Im Neuenheimer Feld 223, 69120 Heidelberg, Germany

[c]Department of Chemistry, Faculty of Science, Masaryk University, Kamenice 5, 625 00 Brno, Czech Republic

[d]Helmholtz-Zentrum Dresden-Rossendorf, Institute of Radiopharmaceutical Cancer Research, Bautzner Landstrasse 400, 01328 Dresden, Germany

[e]Technische Universität Dresden, Faculty of Medicine, Centre for Translational Bone, Joint and Soft Tissue Research, Fetscherstrasse 74, 01307 Dresden, Germany

[f]Technische Universität Dresden, University Hospital Carl Gustav Carus, University Center for Orthopaedics and Traumatology, Fetscherstrasse 74, 01307 Dresden, Germany

[g]Technische Universität Dresden, School of Science, Faculty of Chemistry and Food Chemistry, 01069 Dresden, Germany

Table of content

Figure S1. Distribution diagram of H_5te1P^{BP} ……..……..…….. S3

Figure S2. Chemical shift of H_5te1P^{BP} phosphinate ^{31}P NMR signal in strongly alkaline region ……S3

Scheme S1. The equilibrium showing two protonated forms of H_5te1P^{BP} found in the solid state …..S4

Table S1. Comparison of protonation constants of the bis(phosphonate) group ...…….. S4

Table S2. Protonation constants logK_h of the ternary complexes of H_5te1P^{BP} in which Cu^{II} ion is bound in the macrocyclic cavity ……..……. S5

Figure S3. UV-VIS spectra of Cu^{II}-H_5te1P^{BP} system in the strongly acidic region and absorbance at 580 nm as function of pH ……..……..….. S6

Scheme S2. Schematic representation of two six-membered chelate ring formed by bridging methylene-bis(phosphonate) group ...……..……..……. S6

Figure S4. Distribution diagrams of M^{II}-$te1P^{BP}$ binary systems …..……... S7

Figure S5. Distribution diagrams of M^{II}–{Cu^{II}-$te1P^{BP}$} ternary systems …..…….. S9

Figure S6. Spectra of the Cu^{II}-H_5te1P^{BP} system during complexation and absorbance at 273 nm as function of time at a ligand excess ……..……..... S15

Figure S7. Observed formation rate constants as a function of ligand or Cu^{II} concentrations ……...S15

Equations describing Cu^{II} complex formation ……..……..…….. S16

Table S3. Formation rate constants and stability constants of *out-of-cage* complexes in the Cu^{II}-H_5te1P^{BP} system …….. S18

Table S4. Comparison between calculated 99% complexation times of H_5te1P^{BP} and related ligands …….. S18

Figure S8. Rate constants $^{f}k_{ML}$ (**A**), $^{f}k_{M2L}$ (**B**) and $^{f}k_{ML2}$ (**C**) as function of pH ……..… S19

Figure S9. Absorbance at 580 nm as function of time during Cu^{II}-$te1P^{BP}$ complex dissociation …. S20

Table S5. Kinetic parameters of acid-assisted decomplexation of Cu^{II}-$te1P^{BP}$ complex ….. S20

Table S6. Activation parameters of acid-assisted dissociation and dissociation half-lives of pentacoordinated isomers of the Cu^{II}-$te1p^{BP}$ complex and related complexes ……... S20

Table S7. Comparison of dissociation halftimes of Cu^{II} complexes with cyclam based ligands ….. S21

Chart S1. Structures of ligands listed in Table S8 ……..… S22

Figure S10. NMR spectra of H_5te1P^{BP} ……..……...…….. S23

Table S8. Experimental crystallographic data for the crystal structure of $H_5te1P^{BP}\cdot 6H_2O$ ……... S24

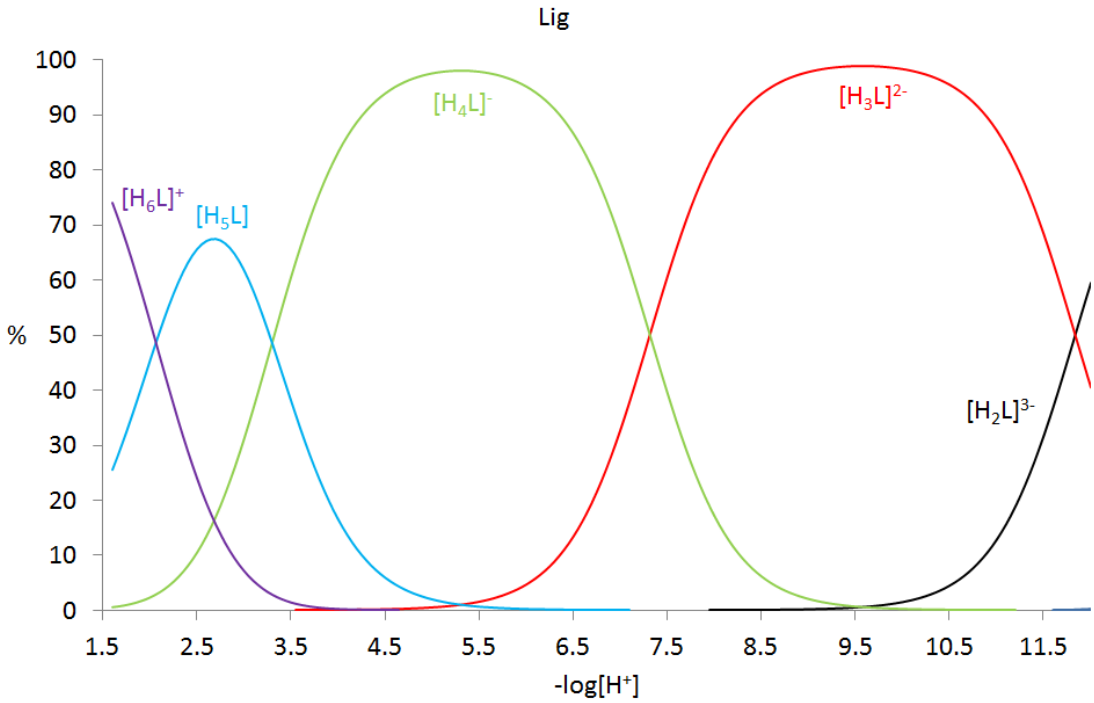

Figure S1. Distribution diagram of H_5te1P^{BP}; I = 0.1 M (NMe_4)Cl, 25 °C.

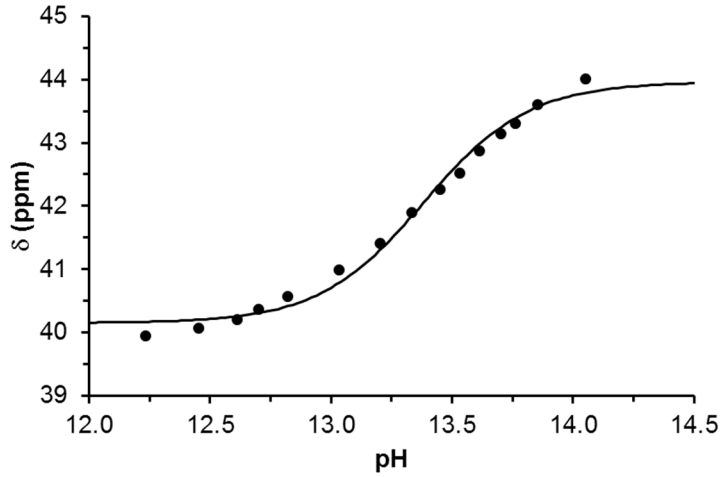

Figure S2. Chemical shift of the H_5te1P^{BP} phosphinate ^{31}P NMR signal in the strongly alkaline region; the line represents the best fit, giving constant logβ_2 shown in Table S1 (c_L = 4 mM).

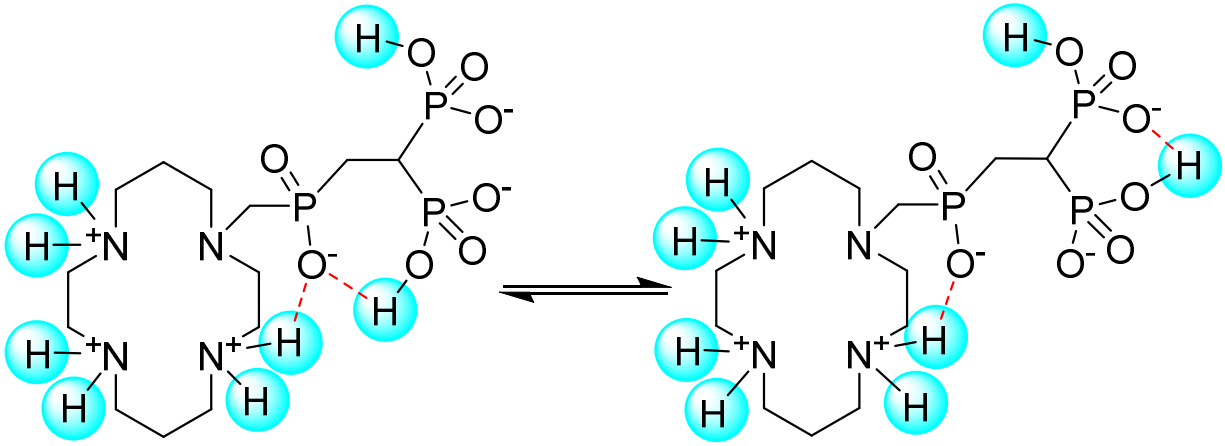

Scheme S1. The equilibrium showing two protonated forms of H_5te1P^{BP} found as a disorder in the solid-state. Hydrogen bonds are shown in red.

Table S1. Comparison of protonation constants of the bis(phosphonate) group

Complex/ligand	logK_1	logK_2	logK_3	logK_4
Cu^{II}-te1P^{BP} [a]	12.69	7.44	3.46	–
Yb^{III}-dotam^{BP} [b,c]	> 13	9	4.9	1.8
Yb^{III}-do3aP^{BP} [b,d]	11.2	7.0	[g]	[g]
H_4mdp [e]	10.6	7.05	2.77	1.6
H_4aca [f]	10.7	7.5	5.8	1.4

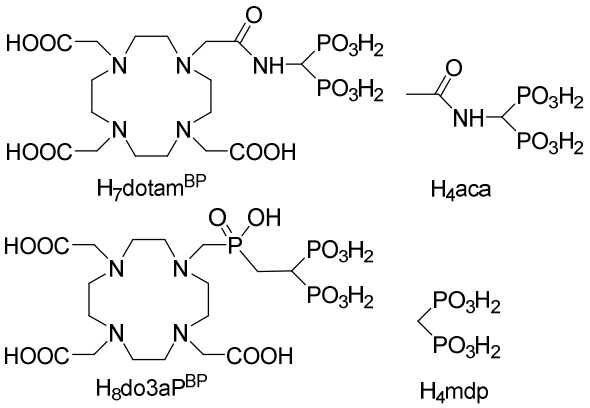

[a]This work. [b]Determined by ^{31}P NMR. [c]Ref. 1. [d]Ref. 2. [e]Ref. 3. [f]Ref.[4] [g]Not determined due to signal broadening.

[1] Vitha, T.; Kubíček, V.; Hermann, P.; Vander Elst, L.; Muller, R. N.; Kolar, Z. I.; Wolterbeek, H. T.; Breeman, W. A. P.; Lukeš, I.; Peters, J. A. Lanthanide(III) complexes of bis(phosphonate) monoamide analogues of DOTA: Bone-seeking agents for imaging and therapy. *J. Med. Chem.* **2008**, *51*, 677–683.

[2] Vitha, T.; Kubíček, V.; Kotek, J.; Hermann, P.; Vander Elst, L.; Muller, R. N.; Lukeš, I.; Peters, J. A. A Gd(III) complex of a monophosphinate-bis(phosphonate) DOTA analogue with a high ^{1}H NMR relaxivity: Lanthanide(III) complexes for imaging and radiotherapy of calcified tissues. *Dalton Trans.* **2009**, 3204–3214.

[3] NIST Standard Reference Database 46 (Critically Selected Stability Constants of Metal Complexes), Version 7.0, 2003.

[4] Kubíček, V.; Kotek, J.; Hermann, P.; Lukeš, I. Aminoalkylbis(phosphonates): Their complexation properties in solution and in the solid state. *Eur. J. Inorg. Chem.* **2007**, 333–344.

Table S2. Protonation constants logK_h of the ternary complexes of H_5te1P^{BP} in which the Cu^{II} ion is bound in the macrocyclic cavity (I = 0.1 M NMe_4Cl, 25 °C)

Equilibrium[b]	Cu^{II}	Zn^{II}	Ca^{II}	Mg^{II}
{M[Cu(L)]} + H → {M[Cu(HL)]}	6.05	2 × 5.30 [a]	9.51	8.97
{M[Cu(HL)]} + H → {M[Cu(H_2L)]}	4.03		6.22	6.06
{M(OH)[Cu(L)]} + H → {M[Cu(L)]}	2 × 10.77 [a]	9.92	–	–
{M(OH)$_2$[Cu(L)]}+ H → {M(OH)[Cu(L)]}		12.07	–	–
{M$_2$(OH)[Cu(L)]} + H → {M$_2$[Cu(L)]}	5.36	7.08	–	10.62
{M$_2$(OH)$_2$[Cu(L)]} + H → {M$_2$(OH)[Cu(L)]}	9.12	9.81	–	12.44
{M$_2$(OH)$_3$[Cu(L)]} + H → {M$_2$(OH)$_2$[Cu(L)]}	11.43	10.12	–	–
{M[Cu(L)]$_2$} + H → {M[Cu(L)][Cu(HL)]}	2 × 8.46 [a]	2 × 8.99 [a]	12.6	–
{M[Cu(L)][Cu(HL)]} + H → {M[Cu(HL)]$_2$}			8.61	–

[a]Protonation over two steps. [b]Charges are omitted.

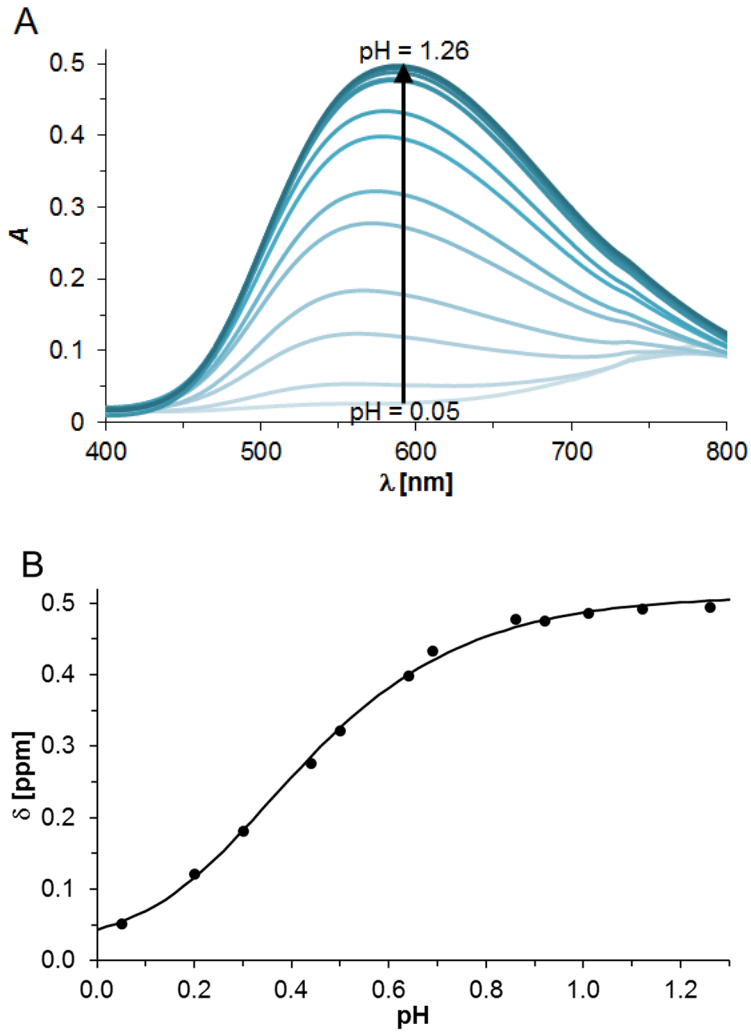

Figure S3. UV-VIS spectra of Cu^{II}-H_5te1P^{BP} system (c_L = c_{Cu} = 4 mM) in the strongly acidic region (**A**) and UV-VIS absorbance at 580 nm as function of pH (**B**, the line represents the best fit, giving the constants outline in Table S2).

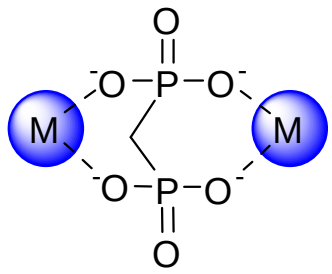

Scheme S2. Schematic representation of two six-membered chelate ring formed by bridging methylene-bis(phosphonate) group. It is common motif in complexes of geminal bis(phosphonate) ligands with the [ML_2] stoichiometry.

Figure S4. Distribution diagrams of M^{II}-H_5te1P^{BP} binary systems (c_M = c_L = 4 mM); I = 0.1 M $(NMe_4)Cl$, 25 °C

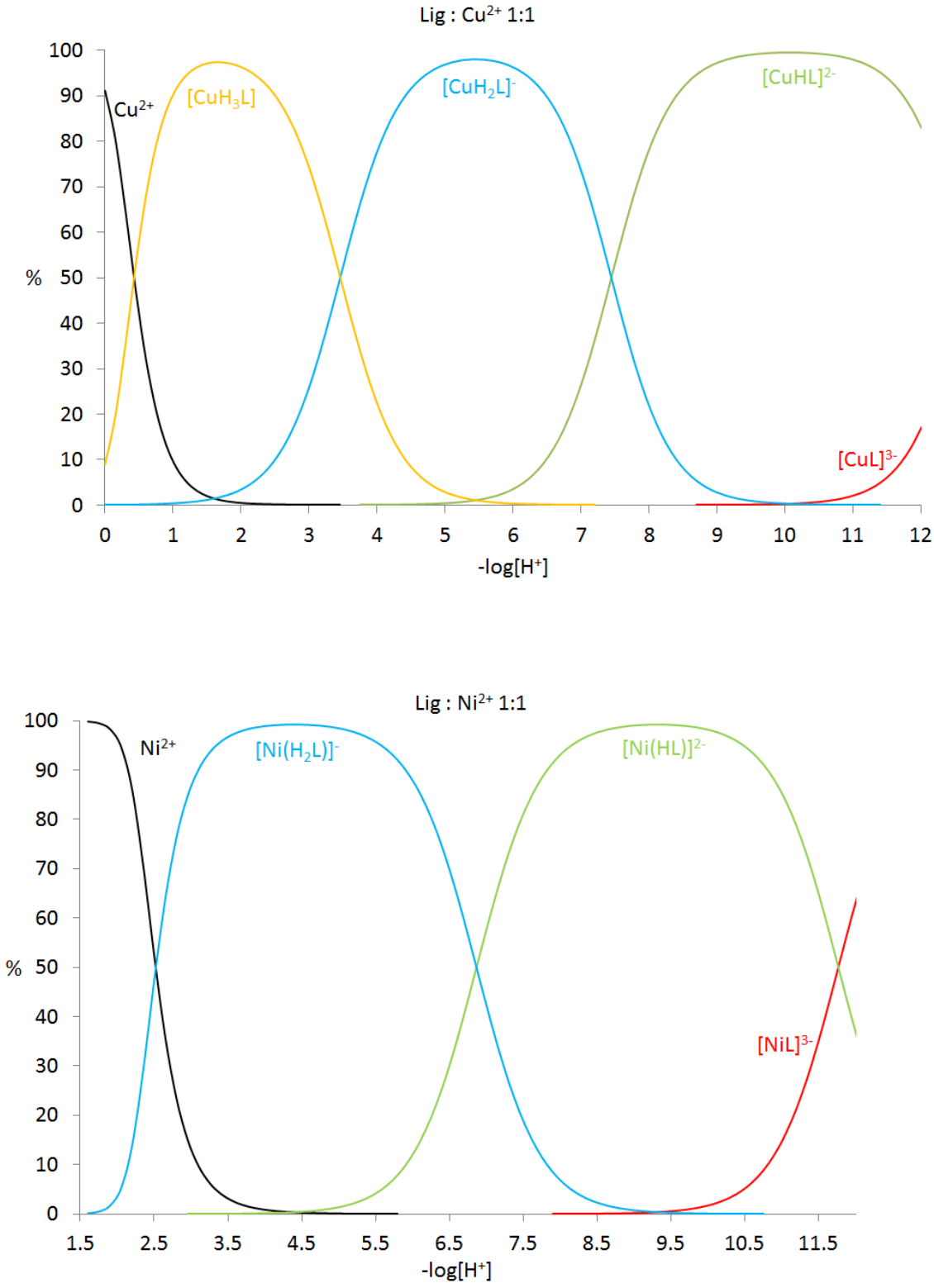

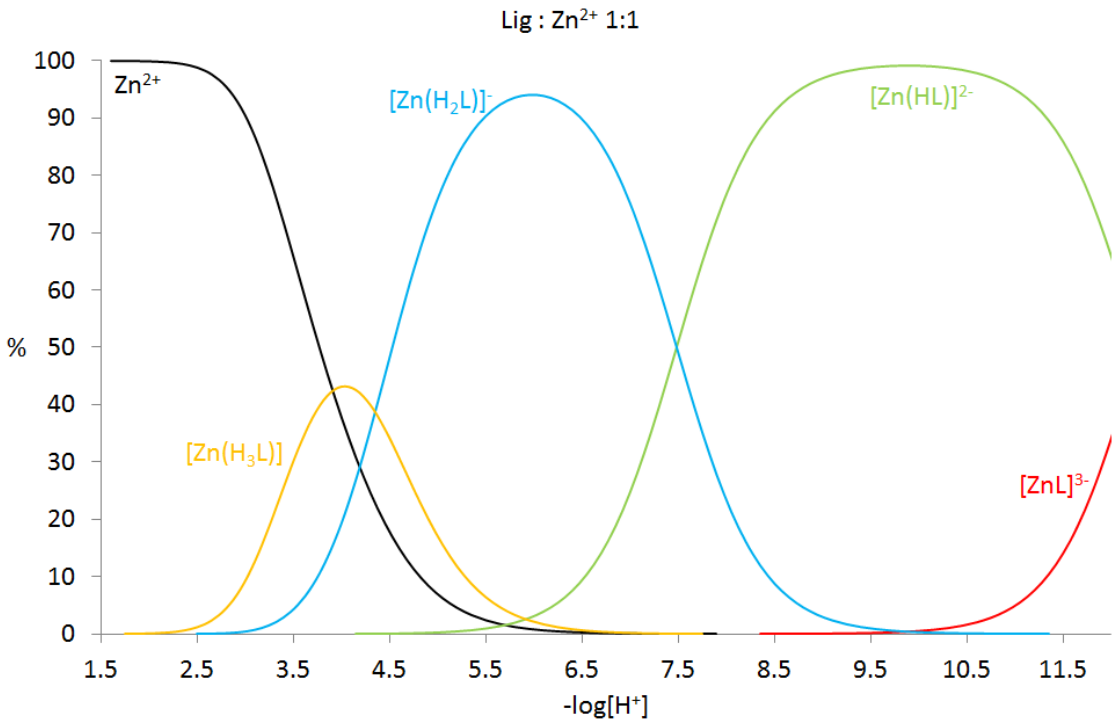
Lig : Zn2+ 1:1
100
90
80
70
60
50
40
30
20
10
0
%
Zn2+
[Zn(H2L)]-
[Zn(HL)]2-
[Zn(H3L)]
[ZnL]3-
1.5
2.5
3.5
4.5
5.5
6.5
7.5
8.5
9.5
10.5
11.5
-log[H+]

Figure S5. Distribution diagrams of M^{II}-{Cu^{II}-te1P^{BP}} ternary systems (c_{CuL} = 4 mM, c_M = 2 mM or 4 mM or 8 mM); I = 0.1 M $(NMe_4)Cl$, 25 °C

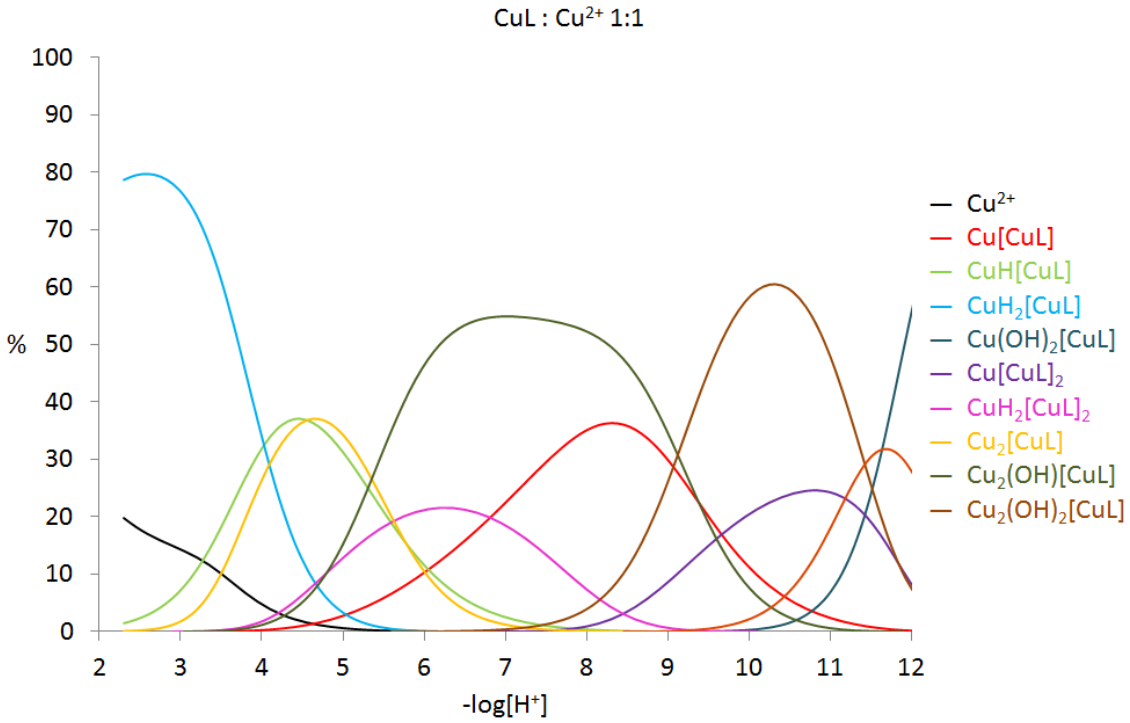

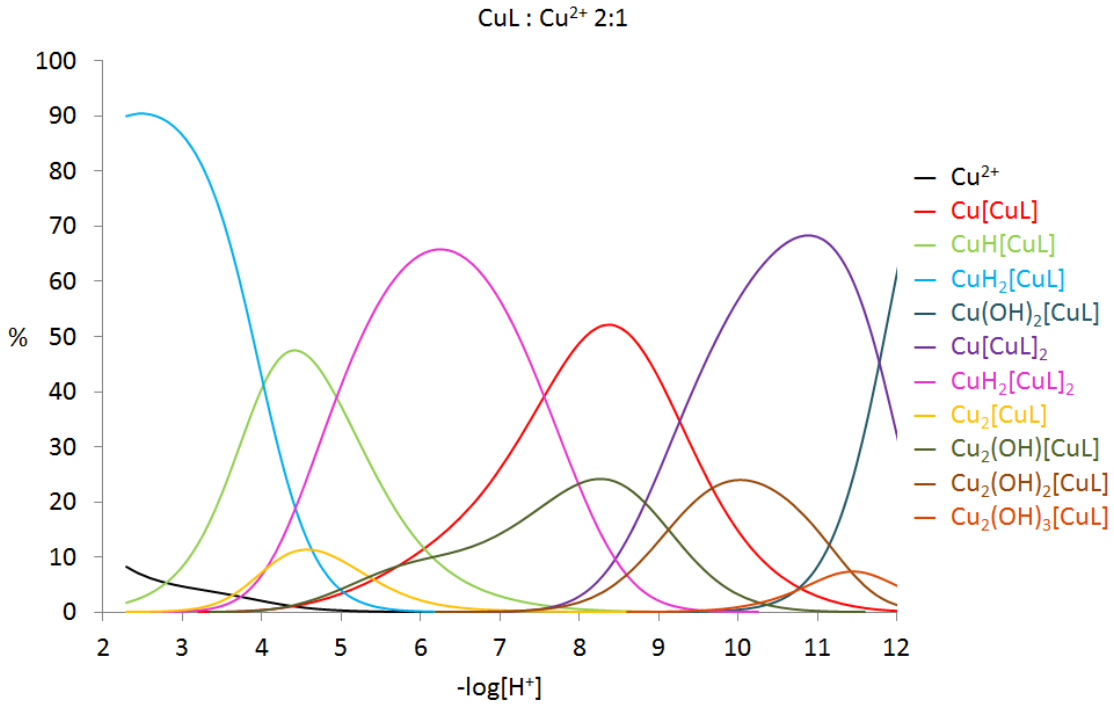

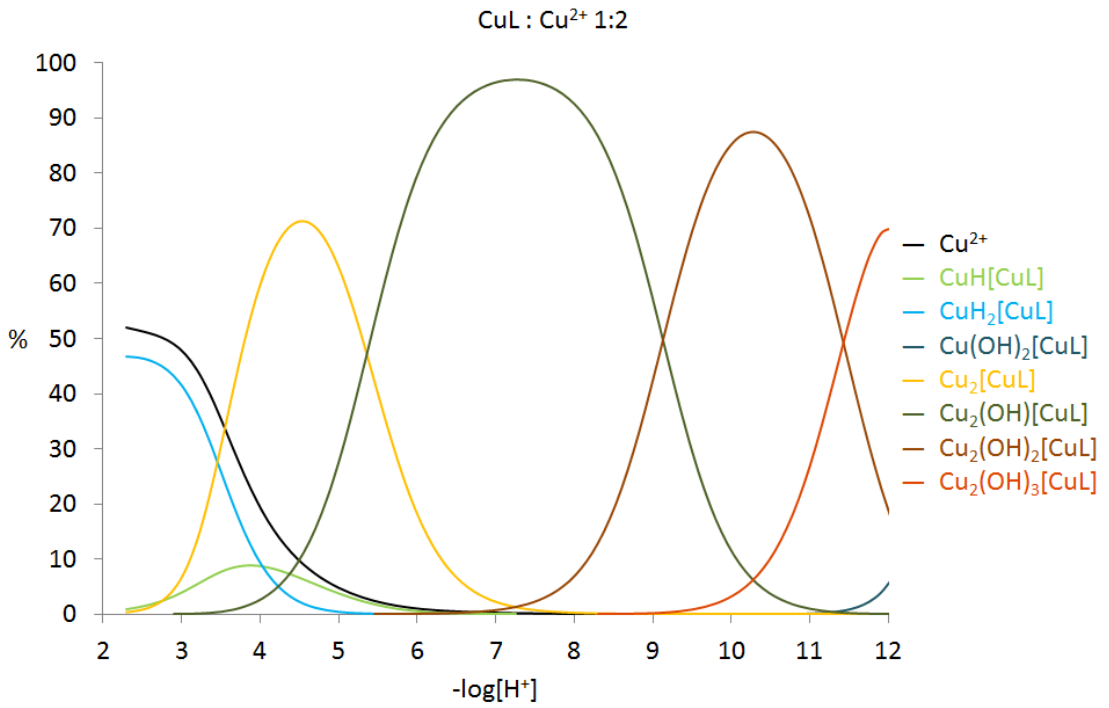
CuL : Cu2+ 1:2
100
90
80
70
60
50
40
30
20
10
0
%
2
3
4
5
6
7
8
9
10
11
12
-log[H+]
Cu2+
CuH[CuL]
CuH2[CuL]
Cu(OH)2[CuL]
Cu2[CuL]
Cu2(OH)[CuL]
Cu2(OH)2[CuL]
Cu2(OH)3[CuL]

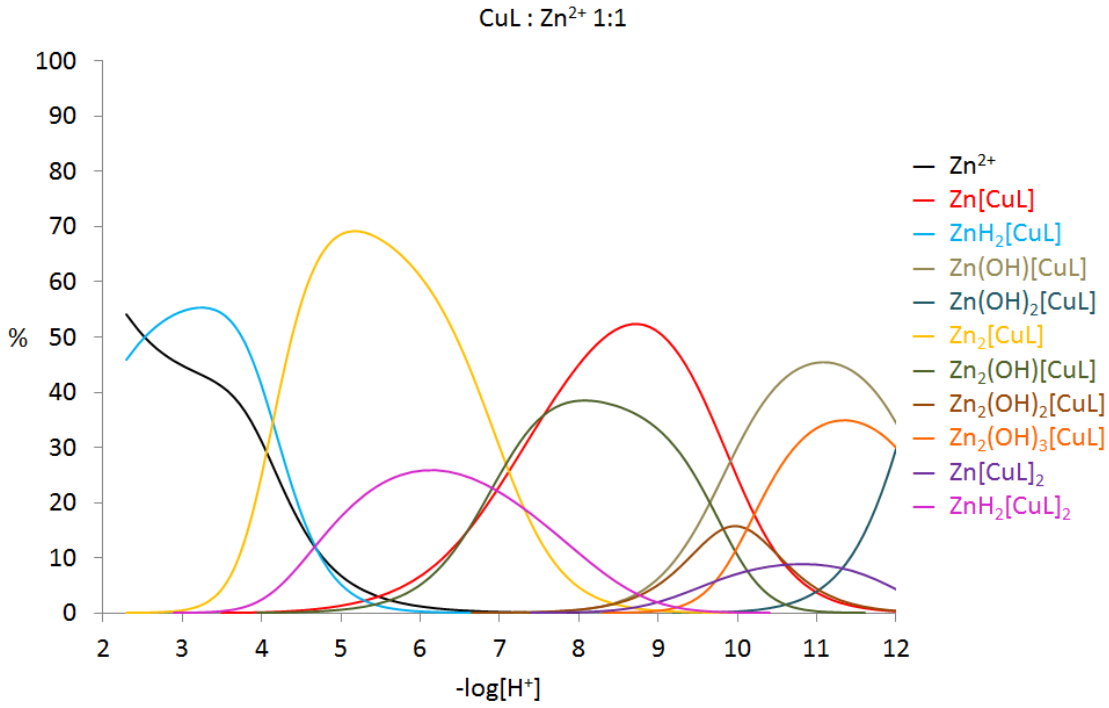
CuL : Zn2+ 1:1
100
90
80
70
60
50
40
30
20
10
0
%
2
3
4
5
6
7
8
9
10
11
12
-log[H+]
Zn2+
Zn[CuL]
ZnH2[CuL]
Zn(OH)[CuL]
Zn(OH)2[CuL]
Zn2[CuL]
Zn2(OH)[CuL]
Zn2(OH)2[CuL]
Zn2(OH)3[CuL]
Zn[CuL]2
ZnH2[CuL]2

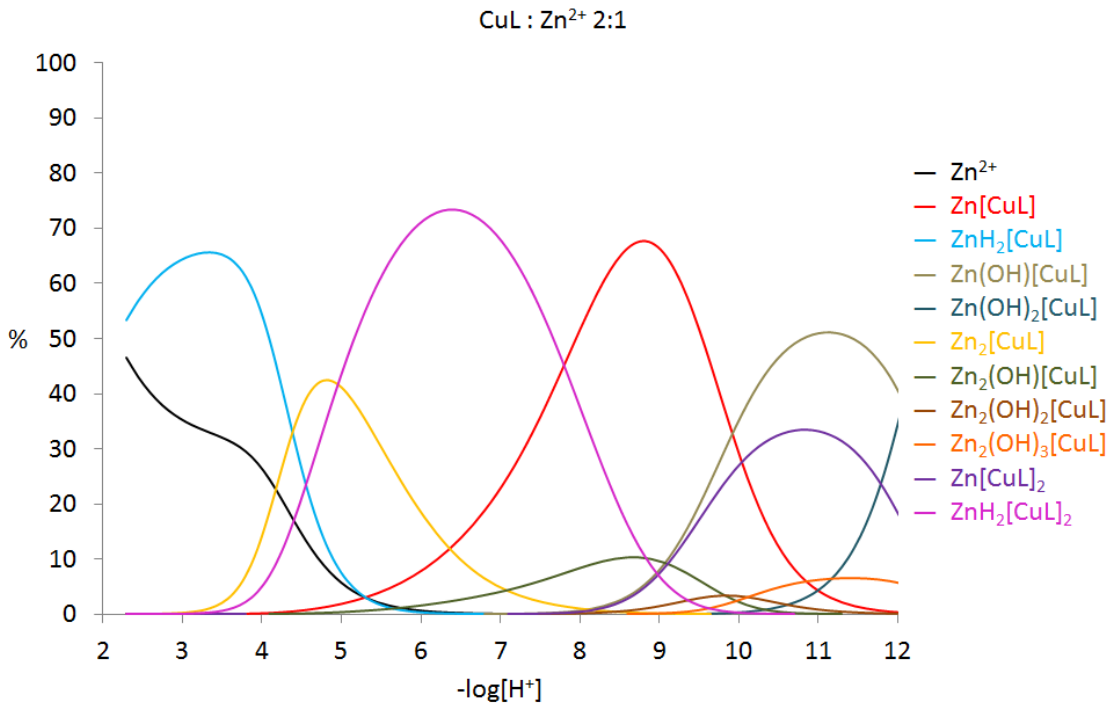
CuL : Zn2+ 2:1
100
90
80
70
60
50
40
30
20
10
0
%
2
3
4
5
6
7
8
9
10
11
12
-log[H+]
Zn2+
Zn[CuL]
ZnH2[CuL]
Zn(OH)[CuL]
Zn(OH)2[CuL]
Zn2[CuL]
Zn2(OH)[CuL]
Zn2(OH)2[CuL]
Zn2(OH)3[CuL]
Zn[CuL]2
ZnH2[CuL]2

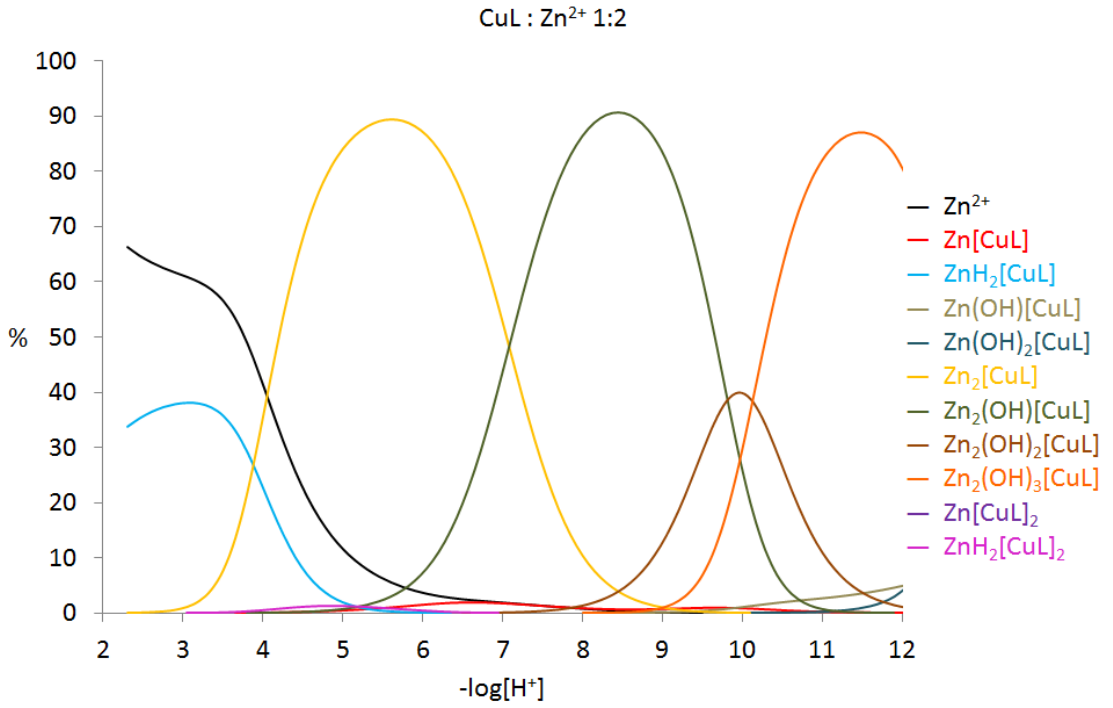
CuL : Zn2+ 1:2
100
90
80
70
60
50
40
30
20
10
0
%
2
3
4
5
6
7
8
9
10
11
12
-log[H+]
Zn2+
Zn[CuL]
ZnH2[CuL]
Zn(OH)[CuL]
Zn(OH)2[CuL]
Zn2[CuL]
Zn2(OH)[CuL]
Zn2(OH)2[CuL]
Zn2(OH)3[CuL]
Zn[CuL]2
ZnH2[CuL]2

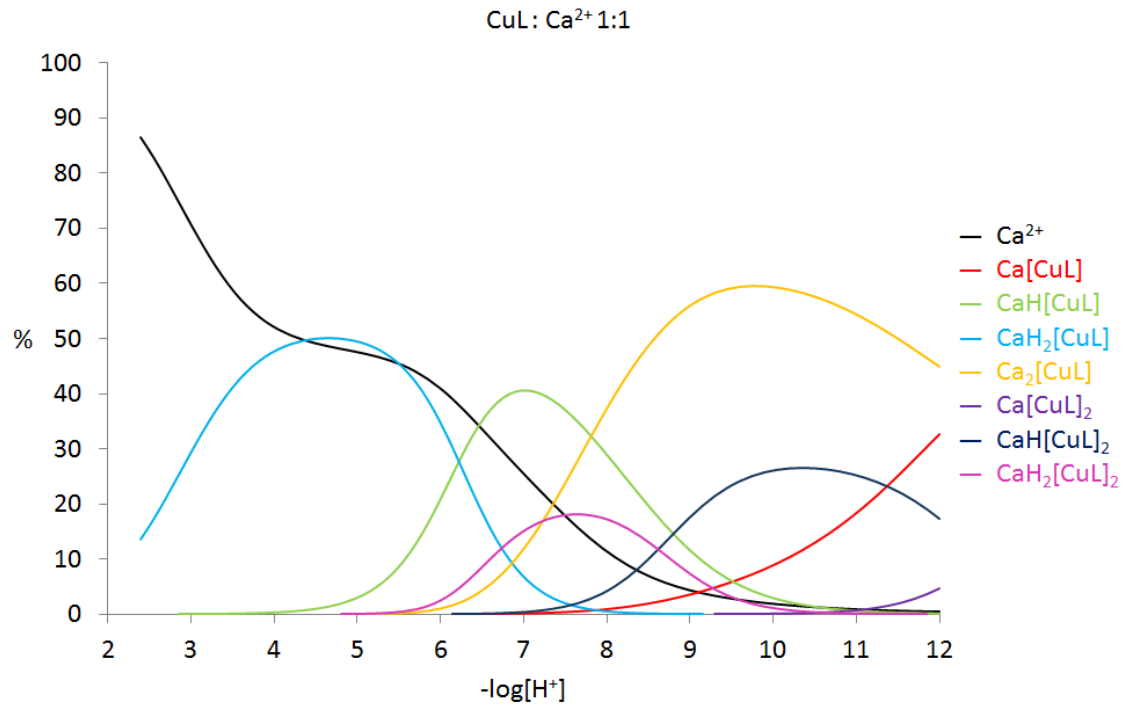
CuL : Ca2+ 1:1
100
90
80
70
60
50
40
30
20
10
0
%
2
3
4
5
6
7
8
9
10
11
12
-log[H+]
Ca2+
Ca[CuL]
CaH[CuL]
CaH2[CuL]
Ca2[CuL]
Ca[CuL]2
CaH[CuL]2
CaH2[CuL]2

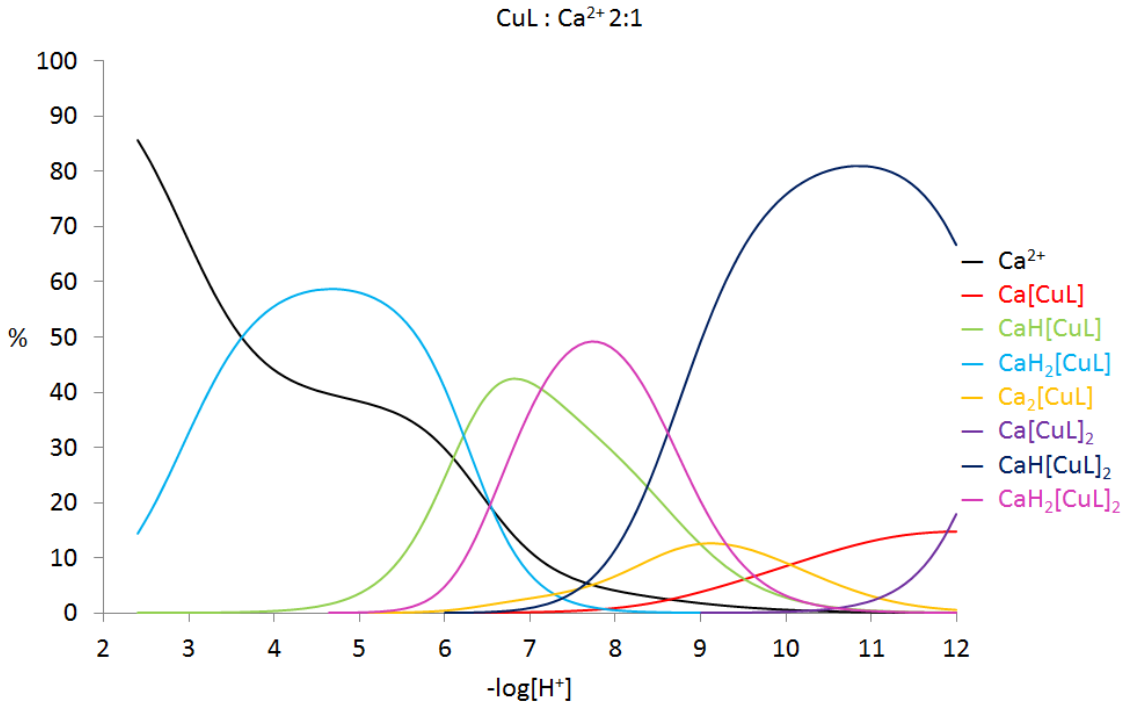
CuL : Ca2+ 2:1
100
90
80
70
60
50
40
30
20
10
0
%
2
3
4
5
6
7
8
9
10
11
12
-log[H+]
Ca2+
Ca[CuL]
CaH[CuL]
CaH2[CuL]
Ca2[CuL]
Ca[CuL]2
CaH[CuL]2
CaH2[CuL]2

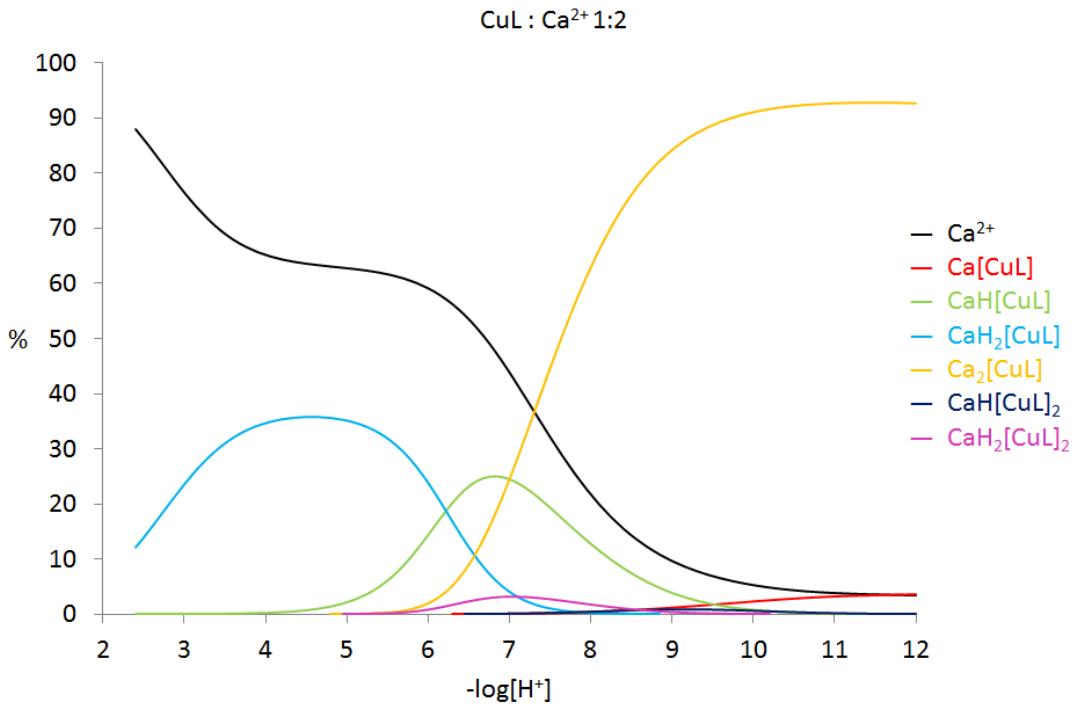
CuL : Ca2+ 1:2
100
90
80
70
60
50
40
30
20
10
0
%
2
3
4
5
6
7
8
9
10
11
12
-log[H+]
Ca2+
Ca[CuL]
CaH[CuL]
CaH2[CuL]
Ca2[CuL]
CaH[CuL]2
CaH2[CuL]2

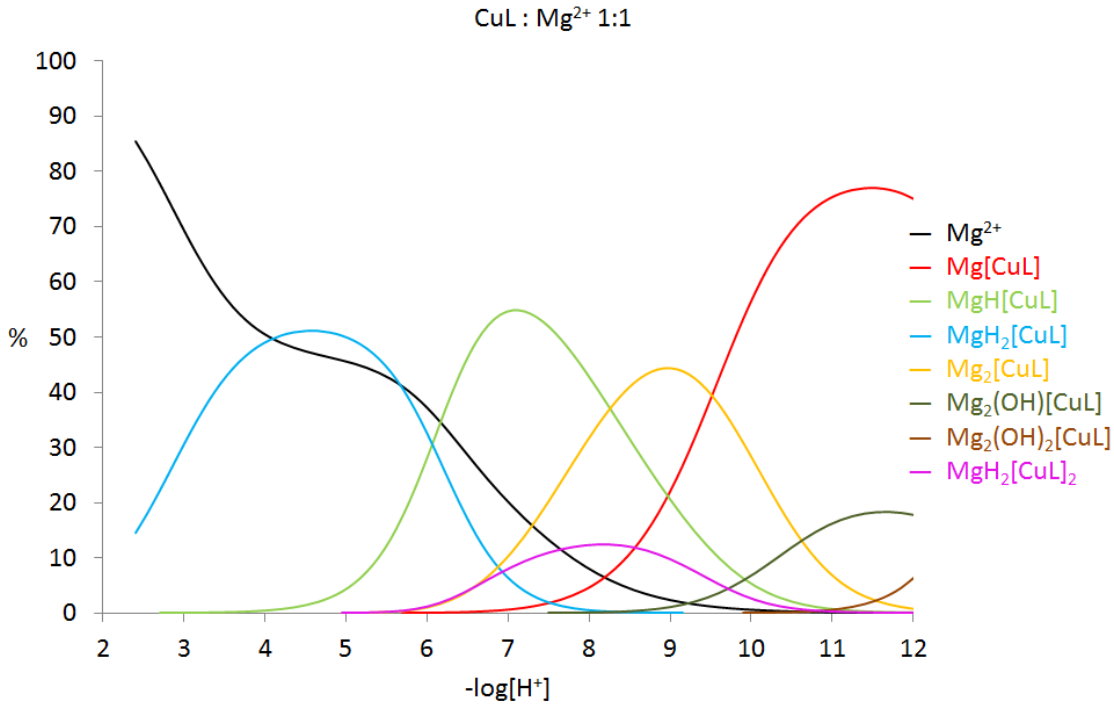
CuL : Mg2+ 1:1
100
90
80
70
60
50
40
30
20
10
0
%
2
3
4
5
6
7
8
9
10
11
12
-log[H+]
Mg2+
Mg[CuL]
MgH[CuL]
MgH2[CuL]
Mg2[CuL]
Mg2(OH)[CuL]
Mg2(OH)2[CuL]
MgH2[CuL]2

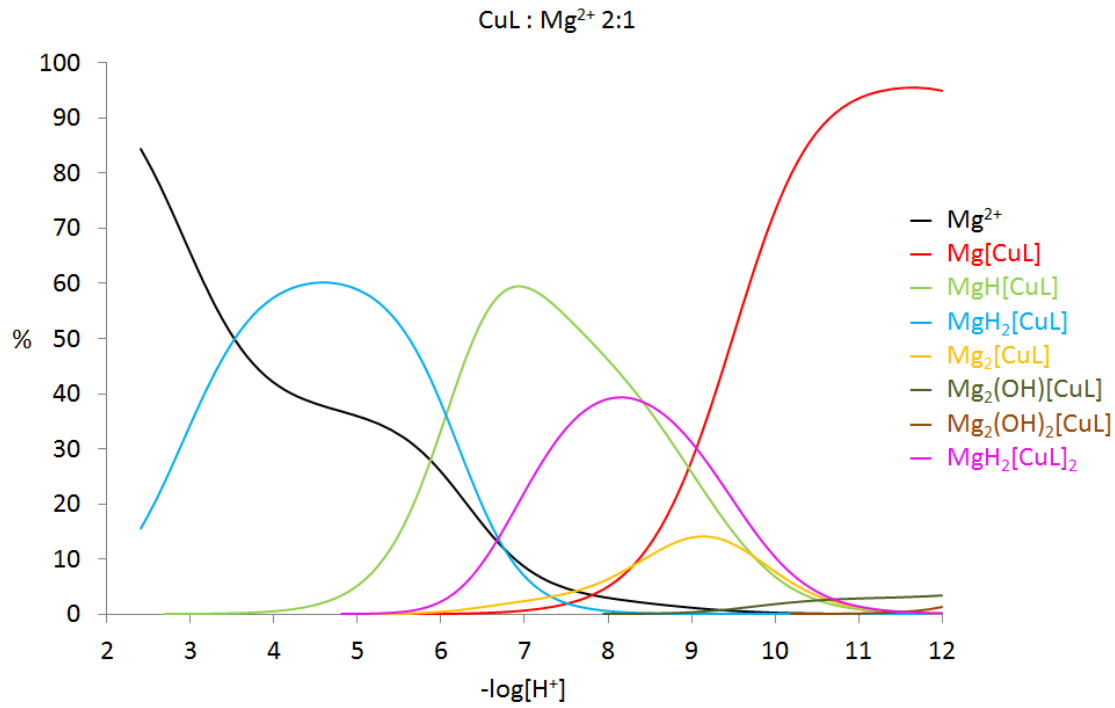
CuL : Mg2+ 2:1
100
90
80
70
60
50
40
30
20
10
0
%
2
3
4
5
6
7
8
9
10
11
12
-log[H+]
Mg2+
Mg[CuL]
MgH[CuL]
MgH2[CuL]
Mg2[CuL]
Mg2(OH)[CuL]
Mg2(OH)2[CuL]
MgH2[CuL]2

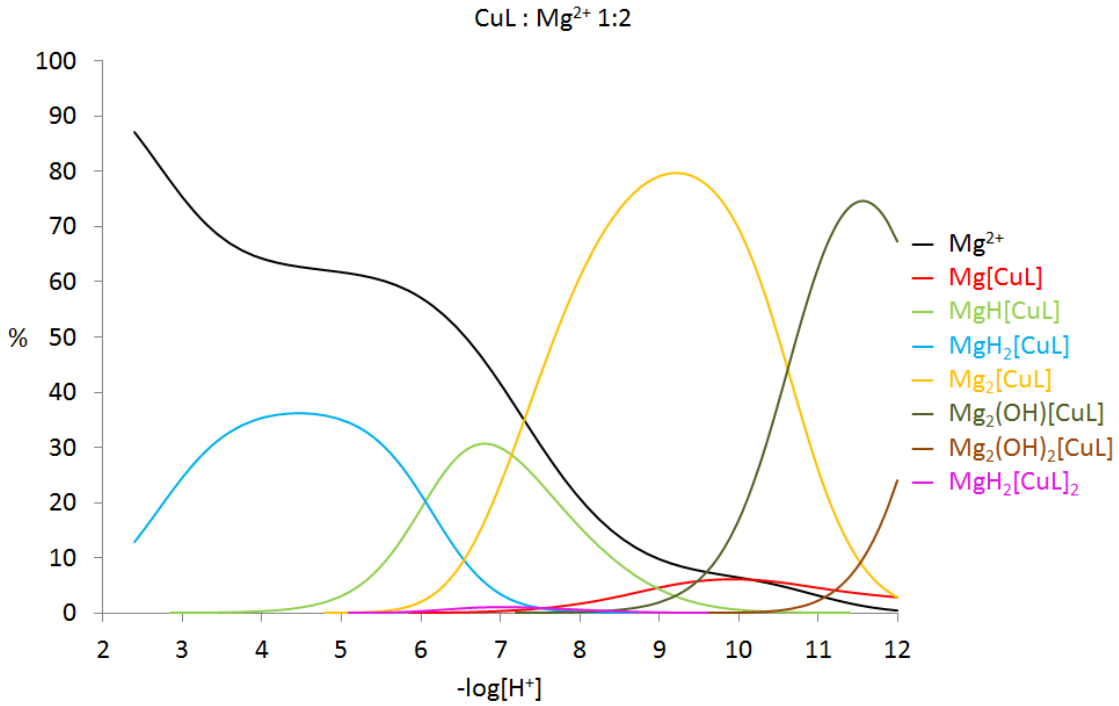
CuL : Mg2+ 1:2
100
90
80
70
60
50
40
30
20
10
0
%
2
3
4
5
6
7
8
9
10
11
12
-log[H+]
Mg2+
Mg[CuL]
MgH[CuL]
MgH2[CuL]
Mg2[CuL]
Mg2(OH)[CuL]
Mg2(OH)2[CuL]
MgH2[CuL]2

A

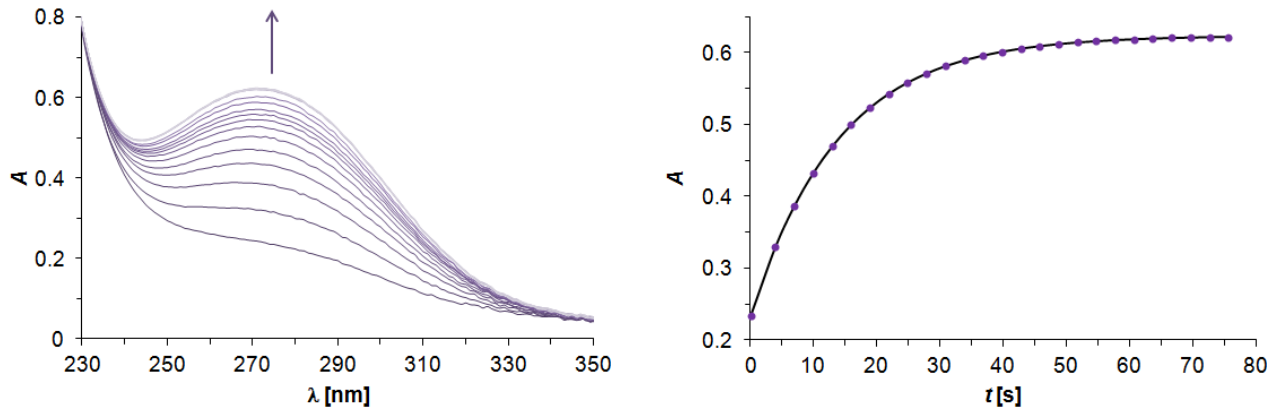

B

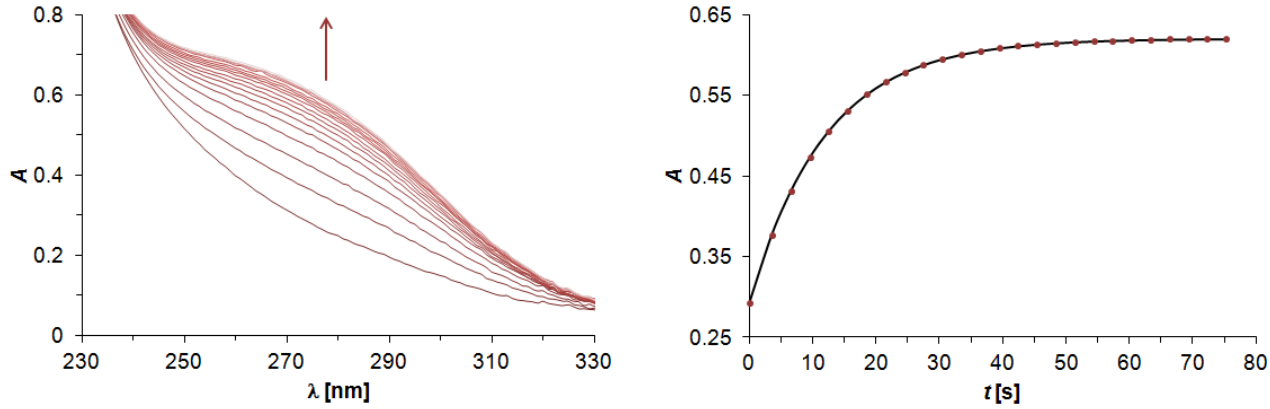

Figure S6. Spectra of the Cu^{II}-H_5te1P^{BP} system during complexation (pH = 3.54, I = 0.1 M KCl, 25 °C) and absorbance at 273 nm as function of time at a ligand excess (**A**, c_L = 0.25 mM, c_M = 0.05 mM) and at a Cu^{II} ion excess (**B**, c_L = 0.05 mM, c_M = 0.25 mM); the lines represent the best fit according to Equation 4.

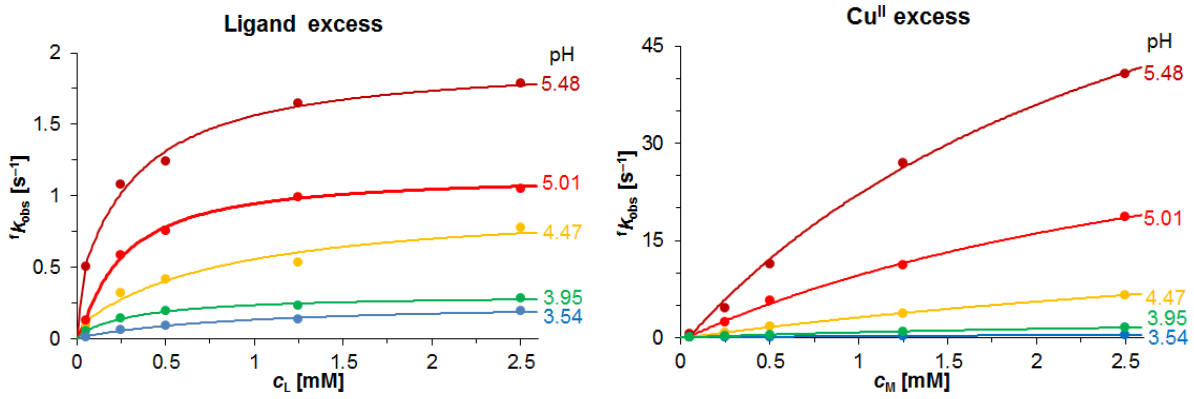

Figure S7. Observed formation rate constants (I = 0.1 M KCl, 25 °C) as a function of ligand (left, c_M = 0.05 mM) or Cu^{II} (right, c_L = 0.05 mM) concentrations; the lines represent the best fits using Equations 1, 2, S1 and S2 and the parameters outlined in Table S3.

Equations describing Cu^{II} complex formation

Macrocyclic complexes with coordinating pendant arms are formed in two steps. An *out-of-cage* complex (indicated in the formulas below with superscript "oc") is immediately formed in the first equilibrium step. In the complex, donor atoms of the pendant arms are coordinated to the metal ion, two macrocyclic amines are protonated, and the protons block access to the macrocyclic cavity. In the next (rate-determining) step, nitrogen atoms of the macrocycle are deprotonated, and the metal ion is simultaneously transferred to the macrocyclic cavity, thus forming the *in-cage* complex (indicated in the formulas below with superscript "ic").

Because bis(phosphonate) is a strongly complexing pendant group, H_4te1P^{BP} forms different types of *out-of-cage* complexes under ligand vs. metal ion excesses. Cu^{II} complexes with bis(phosphonates) are quantitatively formed at pH > 3 even at equimolar amounts at milimolar concentrations. Hence, the 1:1 *out-of-cage* complex $[M(L)]^{oc}$ is quantitatively formed over the entire pH range. In addition, bis(phosphonates) form dinuclear complexes $[M_2(L)]^{oc}$ and complexes with two coordinated ligands $[M(L)_2]^{oc}$ under a metal and ligand excess, respectively (Scheme 1).

The rate of the overall complexation reaction forming the *in-cage* complex can be expressed as a sum of contributions of all expected *out-of-cage* intermediates to the overall transformation into the *in-cage* complex. Then the reaction rate under the metal excess and the ligand excess are shown in Equations 1 and 2, respectively (different protonation states of the ligand in the *out-of-cage* complexes are not shown),

$$\frac{\mathrm{d}[\mathrm{ML}]^{ic}}{\mathrm{d}t} = {}^{f}k_{obs} \cdot [\mathrm{L}]_{tot} = {}^{f}k_{ML} \cdot [\mathrm{M(L)}]^{oc} + {}^{f}k_{M2L} \cdot [\mathrm{M_2(L)}]^{oc} \quad (1)$$

$$\frac{\mathrm{d}[\mathrm{ML}]^{ic}}{\mathrm{d}t} = {}^{f}k_{obs} \cdot [\mathrm{M}]_{tot} = {}^{f}k_{ML} \cdot [\mathrm{M(L)}]^{oc} + {}^{f}k_{ML2} \cdot [\mathrm{M(L)_2}]^{oc} \quad (2)$$

where ${}^{f}k_{obs}$ is the observed reaction rate, $[L]_{tot}$ and $[M]_{tot}$ are overall concentrations of the ligand and metal ion, respectively, and ${}^{f}k_{ML}$, ${}^{f}k_{ML2}$ and ${}^{f}k_{M2L}$ are formation rate constants for the transformation of the corresponding *out-of-cage* complexes into the *in-cage* complex. Quantitative formation of $[M(L)]^{oc}$ species is presumed to occur even at a 1:1 metal-to-ligand ratio, and the equilibrium concentrations of $[M(L)_2]^{oc}$ and $[M_2(L)]^{oc}$ species are expressed by Equations S1 and S2, respectively,

$$[\mathrm{M(L)_2}]^{oc} = K_{ML2} \cdot [\mathrm{M(L)}]^{oc} \cdot [\mathrm{L}] \quad (S1)$$

$$[\mathrm{M_2(L)}]^{oc} = K_{M2L} \cdot [\mathrm{M(L)}]^{oc} \cdot [\mathrm{M}] \quad (S2)$$

where K_{ML2} and K_{M2L} are the conditional stability constants of the *out-of-cage* intermediates (Scheme 1) and [L] and [M] are equilibrium concentrations of the free ligand and metal ion, respectively. Finally, the data were treated to Equations 1, 2, S1 and S2 combined with metal and ligand mass balance equations (Equations S3 and S4) to meet the minimization criterion for the overall fit. For the experiments performed under a ligand excess, only $[M(L)]^{oc}$ and $[M(L)_2]^{oc}$ species were considered, calculating the constants ${}^{f}k_{ML}$, ${}^{f}k_{ML2}$ and K_{ML2} . For the experiments performed under a metal ion excess, only $[M(L)]^{oc}$ and $[M_2(L)]^{oc}$ species were considered, calculating the constants ${}^{f}k_{ML}$, ${}^{f}k_{M2L}$ and K_{M2L}. The constant ${}^{f}k_{ML}$ was determined from both experiments. Thus, two data sets are presented in Figure S4A, which match and therefore support our model.

$$[M]_{tot} = [M] + [M(L)]^{oc} + 2\times[M_2(L)]^{oc} + [M(L)_2]^{oc} \quad \text{(S3)}$$

$$[L]_{tot} = [L] + [M(L)]^{oc} + [M_2(L)]^{oc} + 2\times[M(L)_2]^{oc} \quad \text{(S4)}$$

Table S3. Formation rate constants and stability constants of *out-of-cage* complexes in the Cu^{II}-H_5te1P^{BP} system (I = 0.1 M KCl, 25 °C)

	pH	$^{f}k_{ML}$ [s^{-1}]	$^{f}k_{M2L}$ [s^{-1}]	K_{M2L} [M^{-1}]	log{K_{M2L} /M^{-1}}
Metal excess	3.54	$(1.8\pm1.3)\times10^{-2}$	$(9\pm2)\times10^{-2}$	$(3.3\pm1.3)\times10^{2}$	2.51 ± 0.17
	3.95	$(7\pm2)\times10^{-2}$	3.8±0.3	$(2.7\pm0.4)\times10^{2}$	2.43 ± 0.06
	4.47	$(7\pm3)\times10^{-2}$	23±2	$(1.7\pm0.2)\times10^{2}$	2.23 ± 0.05
	5.01	$(2\pm3)\times10^{-1}$	45±7	$(2.8\pm0.7)\times10^{2}$	2.45 ± 0.11
	5.48	$(4\pm2)\times10^{-1}$	88±15	$(3.5\pm1.1)\times10^{2}$	2.54 ± 0.14

	pH	$^{f}k_{ML}$ [s^{-1}]	$^{f}k_{ML2}$ [s^{-1}]	K_{ML2} [M^{-1}]	log{K_{ML2} /M^{-1}}
Ligand excess	3.54	$(1.7\pm0.9)\times10^{-2}$	$(2.6\pm0.3)\times10^{-1}$	$(1.0\pm0.3)\times10^{3}$	3.00 ± 0.13
	3.95	$(5.0\pm1.0)\times10^{-2}$	$(3.1\pm0.2)\times10^{-1}$	$(2.7\pm0.8)\times10^{3}$	3.43 ± 0.13
	4.47	$(1.2\pm0.7)\times10^{-1}$	0.9±0.2	$(1.2\pm0.8)\times10^{3}$	3.08 ± 0.29
	5.01	$(1.3\pm0.3)\times10^{-1}$	1.2±0.1	$(4.1\pm0.9)\times10^{3}$	3.61 ± 0.10
	5.48	$(5.2\pm10)\times10^{-1}$	2.0±0.3	$(2.9\pm1.6)\times10^{3}$	3.47 ± 0.24

Table S4. Comparison of calculated 99% complexation times (c_L = 0.05 mM, c_{Cu} = 0.5 mM, 25 °C) of H_5te1P^{BP} and related ligands

Ligand	Ref.	pH 4	pH 5	pH 6
H_5te1P^{BP}	this work	10 s	1 s	0.1 s [a]
H_4te2P	5	64 s	3 s	0.2 s
H_2te1P^{PIN}	6	16 s	2 s	0.2 s
H_4cb-te2P	7	3.6 h	3.4 min	3 s
H_4cb-te2P^{PIN}	7	14 s	3 s	1 s

[a]Extrapolated.

[5] Kotek, J.; Lubal, P.; Hermann, P.; Císařová, I.; Lukeš, I.; Godula, T.; Svobodová, I.; Táborský, P.; Havel, J. Unusually High Thermodynamic Stability and Extraordinary Kinetic Inertness of Copper(II) Complexes with 1,4,8,11-Tetraazacyclotetradecane-1,8-bis(methylphosphonic Acid). Example of a Rare Isomerism Between Kinetically Inert Penta- and Hexacoordinated Copper(II) Complexes. *Chem. Eur. J.* **2003**, *9*, 233–248.

[6] David, T.; Kubíček, V.; Gutten, O.; Lubal, P.; Kotek, J.; Pietzsch, H.-J.; Rulíšek, L.; Hermann, P. Cyclam Derivatives with a Bis(phosphinate) or a Phosphinato-Phosphonate Pendant Arm. *Inorg. Chem.* **2015**, *54*, 11751–11766.

[7] Pazderova, L.; David, T.; Hlinová, V.; Plutnar, J.; Kotek, J.; Lubal, P.; Kubíček, V.; Hermann, P. Cross-Bridged Cyclam with Phosphonate and Phosphinate Pendant Arms: Chelators for Copper Radioisotopes with Fast Complexation. *Inorg. Chem.* **2020**, *59*, 8432−8443.

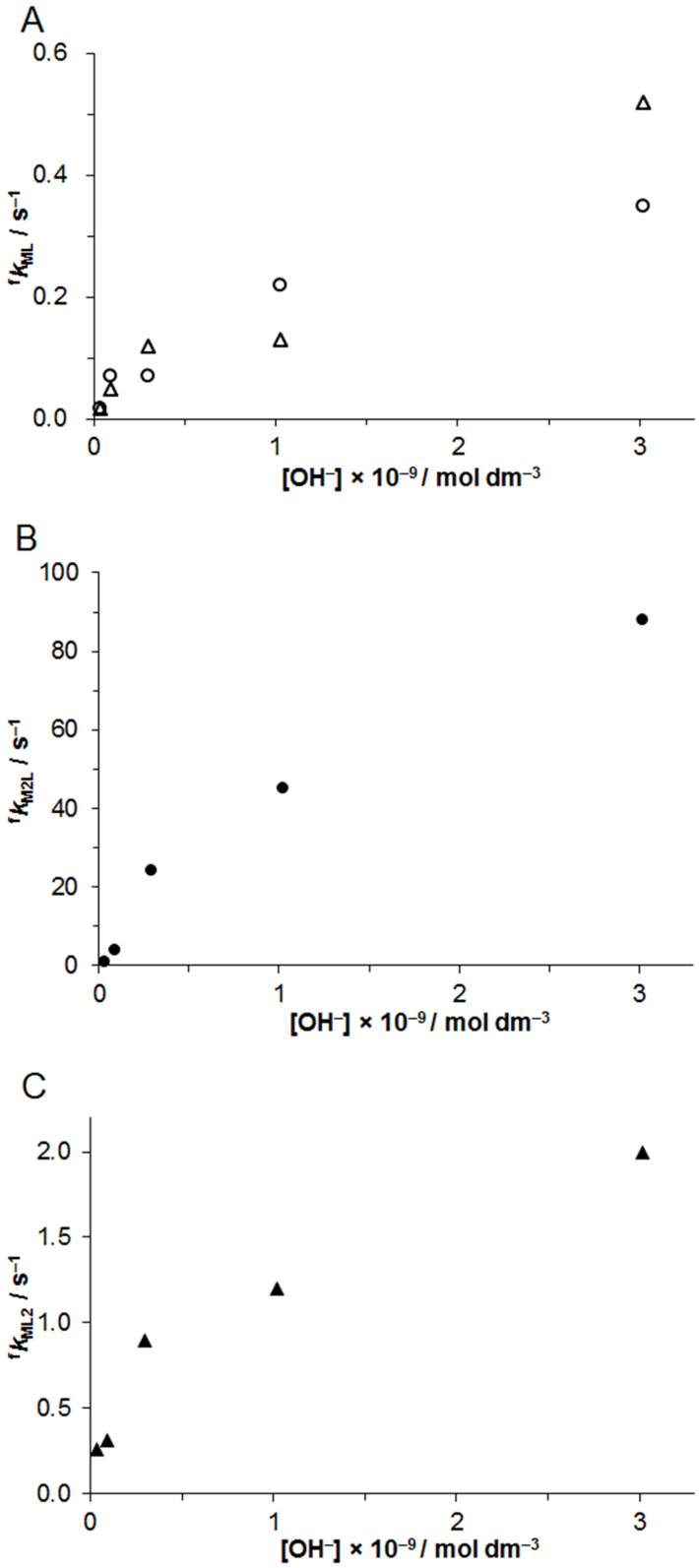

Figure S8. Rate constants $^{f}k_{ML}$ (**A**), $^{f}k_{M2L}$ (**B**) and $^{f}k_{ML2}$ (**C**) as function of pH (I = 0.1 M KCl, 25 °C); empty circles in **A** show values determined from experiments performed under a metal ion excess, and empty triangles in **A** show values determined from experiments performed under a ligand excess. Data points shown in **B** and **C** were calculated from experiments performed under a ligand and metal excess, respectively.

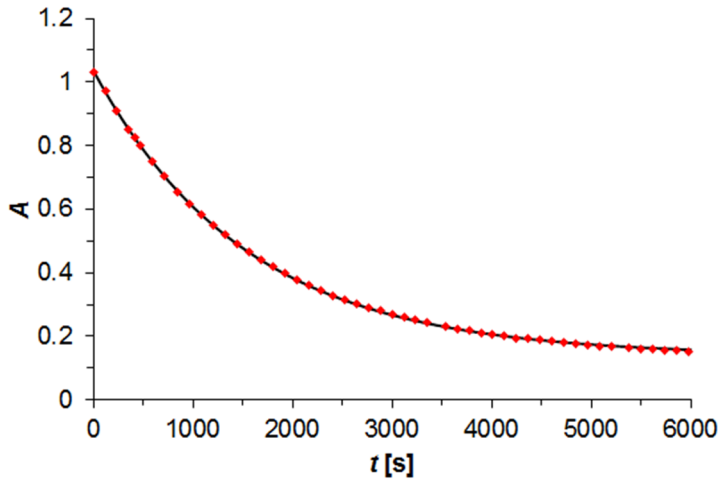

Figure S9. Absorbance at 580 nm as function of time during Cu^{II}-te1P^{BP} complex dissociation (c = 0.1 mM) in 1 M $HClO_4$ at 50 °C (I = 5 M (H/Na)ClO_4); the line represents the best fit according to Equation 4.

Table S5. Kinetic parameters of the acid-assisted decomplexation of Cu^{II}-te1P^{BP} complex.

Parameter	40 °C	50 °C	60 °C	70 °C
^{d}k [s^{-1}]	$(1.0 \pm 0.1)\cdot10^{-3}$	$(2.6 \pm 0.2)\cdot10^{-3}$	$(5.9 \pm 0.6)\cdot10^{-3}$	$(1.4 \pm 0.2)\cdot10^{-2}$
K_H [M^{-1}]	0.4 ± 0.1	0.39 ± 0.09	0.37 ± 0.08	0.28 ± 0.7
$^{d}k_H$ [M^{-1} s^{-1}]	$0.4\cdot10^{-3}$	$1.01\cdot10^{-3}$	$2.18\cdot10^{-3}$	$3.92\cdot10^{-3}$

Table S6. Activation parameters of acid-assisted dissociation and dissociation half-lives of pentacoordinated isomers of the Cu^{II}-te1p^{BP} complex and related complexes.

Parameter	Cu^{II}-te1P^{BP}	Cu^{II}-te1P^{PON}	Cu^{II}-te2P
	This work	Ref. 30	Ref. 37
E_A [kJ mol^{-1}][a]	79.1 ± 0.1	81	72; 85[d]
$\Delta H^{\#}$ [kJ mol^{-1}][b]	76.3 ± 0.8	78	70; 82[d]
$\Delta S^{\#}$ [J K^{-1} mol^{-1}][b]	–59 ± 3	–61	–71; –52[d]
ΔH [kJ mol^{-1}][c]	–9 ± 3	–13.6	–8.3
ΔS [J K^{-1} mol^{-1}][c]	–36 ± 12	–36	–23
$t_{1/2}$ (1 M $HClO_4$, 70 °C)	3.5 min	2.9 min	0.6 min
$t_{1/2}$ (1 M $HClO_4$, 25 °C)	2.7 h	3.3 h	0.3 h

[a]Arrhenius model: $\ln(^{d}k) = -(E_A/RT) + \ln A$. [b]Eyring model: $\ln(^{d}k/T) = -(\Delta H^{\#}/RT) + \Delta S^{\#}/R) + \ln(k_B/h)$. [c]$\ln K = -(\Delta H/RT) + \Delta S/R)$. [d]Data for two dissociation pathways.

Table S7. Comparison of dissociation halftimes of Cu^{II} complexes with cyclam based ligands. Ligand structures are shown in Chart S1.

Ligand	Conditions	Temp.	$t_{1/2}$	Ref.
H_5te1P^{BP}	**1M $HClO_4$**	**25 °C**	**2.7 h**	**this work**
cyclam	1M HNO_3	25 °C	21 min	8
tmc	1M $HClO_4$	25 °C	22 s	9
H_4teta	5 M HCl	30 °C	3.5 d	10
H_4te2P	1 M $HClO_4$	25 °C	20 min	11
H_3te1P^{PON}	1 M $HClO_4$	25 °C	3 h	12
Hte1pa	1 M HCl	25 °C	32 min	13
H_2te1pyp	1 M HCl	25 °C	35 min	14
HMe_3te1a	1 M $HClO_4$	25 °C	11 min	9
H_2Me_3te1P	1 M $HClO_4$	25 °C	15 min	9
H_2Me_3te1P^{PIN}	1 M $HClO_4$	25 °C	7 min	9
H_2cb-te2a	5 M HCl	90 °C	154 h	10
H_4cb-te2P	1 M $HClO_4$	90 °C	120 h	15
Hcb-te1pa	5 M HCl	25 °C	8 h	13
H_2cb-te1pyp	1 M HCl	25 °C	912 min	14
H_3pcb-te1a1P	12M HCl	90 °C	>> 8 d	16

[8] Chen, L.-H.; Chung, C.-S. Steric and Macrocyclic Effects in the Dissociation Kinetics of Cyclic and Open-Chain Tetraamine Complexes of Copper(II) in Strongly Acidic, Aqueous Media. *Inorg. Chem.* **1988**, *27*, 1880–1883.

[9] Paúrová, M.; David, T.; Císařová, I.; Lubal, P.; Hermann, P.; Kotek J. Optimization of the selectivity and rate of copper radioisotope complexation: Formation and dissociation kinetic studies of 1,4,8-trimethylcyclam-based ligands with different coordinating pendant arms. *New J. Chem.* **2018**, *42*, 11908–29.

[10] Woodin, K. S.; Heroux, K. J.; Boswell, C. A.; Wong, E. H.; Weisman, G. R.; Niu, W.; Tomellini, S. A.; Anderson, C. J.; Zakharov, L. N.; Rheingold, A. L. Kinetic Inertness and Electrochemical Behavior of Copper(II) Tetraazamacrocyclic Complexes: Possible Implications for in Vivo Stability. *Eur. J. Inorg. Chem.* **2005**, 4829–4833.

[11] Kotek, J.; Lubal, P.; Hermann, P.; Císařová, I.; Lukeš, I.; Godula, T.; Svobodová, I.; Táborský, P.; Havel, J. Unusually high thermodynamic stability and extraordinary kinetic inertness of copper(II) complexes with 1,4,8,11-tetraazacyclotetradecane-1,8-bis(methylphosphonic acid). Example of a rare isomerism between kinetically inert penta- and hexacoordinated copper(II) complexes. *Chem. Eur. J.* **2003**, *9*, 233–248.

[12] David, T.; Kubíček, V.; Gutten, O.; Lubal, P.; Kotek, J.; Pietzsch, H.-J.; Rulíšek, L.; Hermann P. Cyclam derivatives with a bis(phosphinate) or a phosphinato−phosphonate pendant arm: Ligands for fast and efficient copper(II) complexation for nuclear medical applications. *Inorg. Chem.* **2015**, *54*, 11751–11766**.**

[13] Lima, L. M. P.; Esteban-Gómez, D.; Delgado, R.; Platas-Iglesias, C.; Tripier, R. Monopicolinate Cyclen and Cyclam Derivatives for Stable Copper(II) Complexation. Inorg. Chem. **2012**, *51*, 6916−6927.

[14] Knighton, R. C.; Troadec, T.; Mazan, V.; Le Saëc, P.; Marionneau-Lambot, S.; Le Bihan, T.; Saffon-Merceron, N.; Le Bris, N.; Chérel, M.; Faivre-Chauvet, A.; Elhabiri, M.; J. Charbonnière, L.; Tripier, R. Cyclam-Based Chelators Bearing Phosphonated Pyridine Pendants for ^{64}Cu-PET Imaging: Synthesis, Physicochemical Studies, Radiolabeling, and Bioimaging. *Inorg. Chem.* **2021**, *60*, 2634–2648.

[15] Pazderova, L.; David, T.; Hlinová, V.; Plutnar, J.; Kotek, J.; Lubal, P.; Kubíček, V.; Hermann, P. Cross-Bridged Cyclam with Phosphonate and Phosphinate Pendant Arms: Chelators for Copper Radioisotopes with Fast Complexation. *Inorg. Chem.* **2020**, *59*, 8432–8443.

[16] Dale, A. V.; An, G. I.; Pandya, D. N.; Ha, Y. S.; Bhatt, N.; Soni, N.; Lee, H.; Ahn, H.; Sarkar, S.; Lee, W.; Huynh, P. T.; Kim, J. Y.; Gwon, M.-R.; Kim, S. H.; Park, J. G.; Yoon, Y. R.; Yoo, J. Synthesis and Evaluation of New Generation Cross-Bridged Bifunctional Chelator for ^{64}Cu Radiotracers. *Inorg. Chem.* **2015**, *54*, 8177–8186.

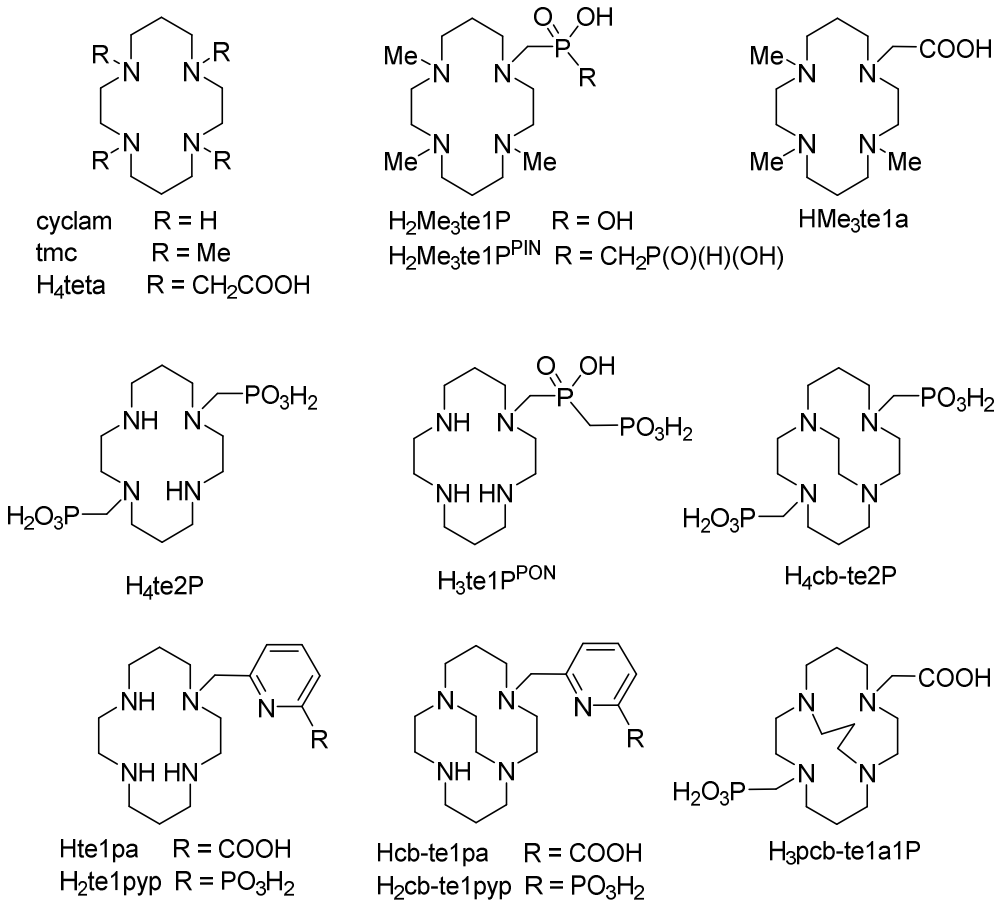

Chart S1. Structures of ligands listed in Table S7.

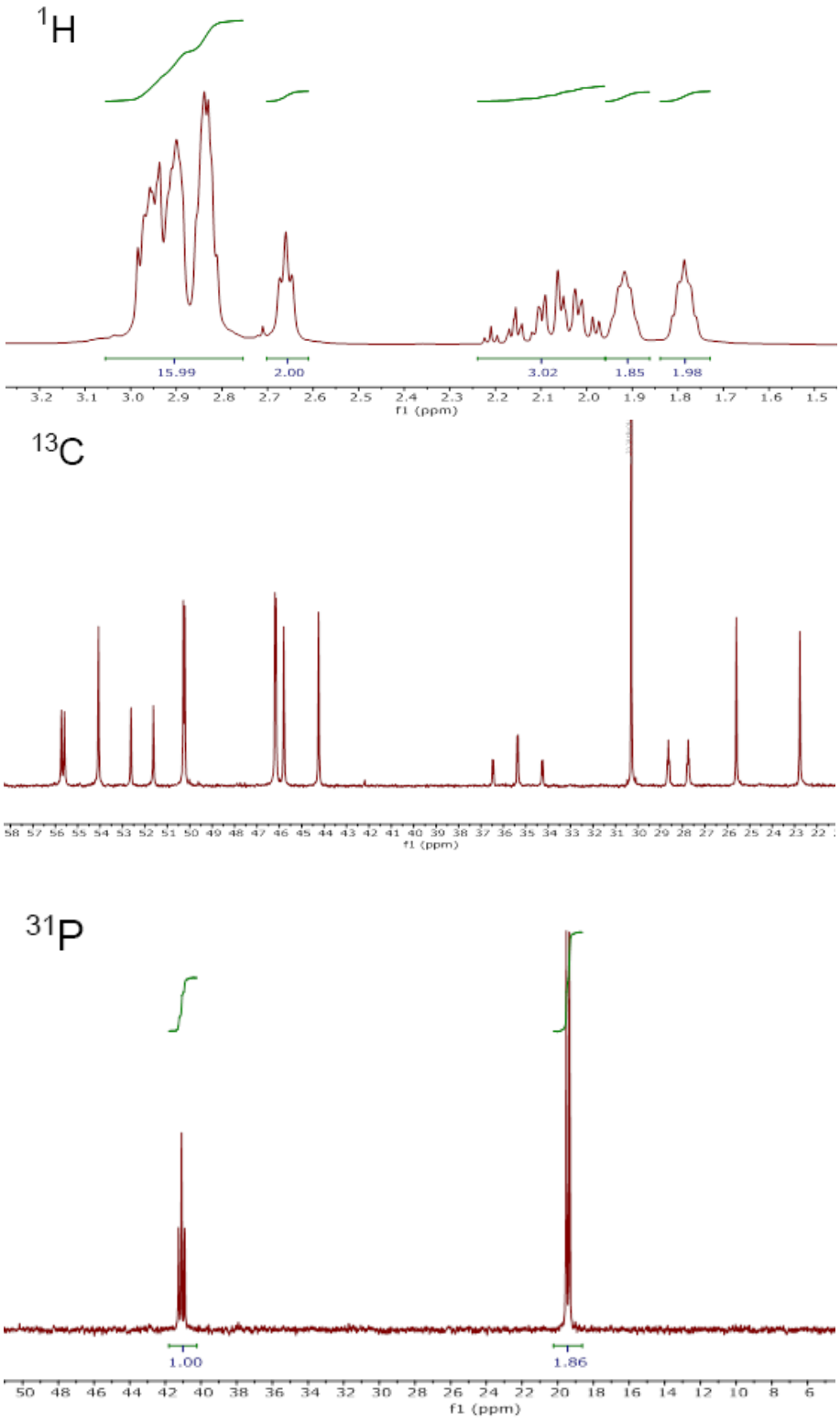

Figure S10. NMR spectra of H_5te1P^{BP} (pH > 12). NMR spectra were measured at high pH as only the deprotonated ligand forms show narrow signals.

Table S8. Experimental crystallographic data for the crystal structure of $H_5te1P^{BP}\cdot 6H_2O$

Parameter	$H_5te1P\cdot 6H_2O$
Formula	$C_{13}H_{45}N_4O_{14}P_3$
M_r	574.44
Habit	bar
Color	colorless
Crystal system	orthorhombic
Space group	P b c a
a, Å	13.2069(4)
b, Å	16.4828(6)
c, Å	22.8799(8)
α, °	90
β, °	90
γ, °	90
U, Å^3	4980.6(3)
Z	8
D_{calc}, g cm^{-3}	1.532
μ, mm^{-1}	2.857
Unique refl.	4397
Obsd. refl. ($I>2s(I)$)	3772
$R(I>2s(I))$	0.0533
R'(all)	0.0619
$wR(I>2s(I))$	0.1403
wR'(all)	0.1463
CCDC number	2086453